

Efficient Reconfiguration of Lattice-Based Modular Robots

Greg Aloupis*

Nadia Benbernou†

Mirela Damian‡

Erik D. Demaine†

Robin Flatland§

John Iacono¶

Stefanie Wuhler||

**Université Libre de Bruxelles, Belgique*†*Massachusetts Institute of Technology, Cambridge, USA*‡*Villanova University, Villanova, USA*§*Siena College, Loudonville, USA*¶*Polytechnic Institute of New York University, USA*||*Carleton University, Ottawa, Canada*

Abstract—Modular robots consist of many small units that attach together and can perform local motions. By combining these motions, we can achieve a reconfiguration of the global shape. The term *modular* comes from the idea of grouping together a fixed number of units into a module, which behaves as a larger individual component.

Recently, a fair amount of research has focused on *Crystalline* robots, whose units (and modules) fit on a cubic lattice. When the proper module size is formed, these robots can reconfigure in linear time within a rather physically restrictive model, or in $O(\log n)$ time in a more unrestricted theoretical model.

In this paper, we show that the results for Crystalline robots also apply to two other modular robots: M-TRAN and Molecube. The common requirement, for each robot type, is that a fixed number of units combine to create modules of specified shapes. In this way, we are able to simulate the actions of Crystalline modules. Previous reconfiguration bounds thus transfer automatically, as long as the robots are composed of the module shapes that we specify.

Index Terms—self-reconfiguring modular robots, cubical units, lattice reconfiguration.

I. INTRODUCTION

A self-reconfiguring modular robot consists of a large number of independent units, or *atoms*, that can arrange themselves into a structure best suited for a given environment or task. For example, a robot may reconfigure into a thin, linear shape to facilitate passage through a narrow tunnel, transform into an emergency structure such as a bridge, or surround and manipulate objects. Because modular robots comprise groups of identical atoms, they are also more easily repaired, by replacing damaged atoms with functional ones. Such robots are well-suited for working in unknown and remote environments.

A variety of atom structures have been designed and prototyped in the robotics community, differing in shape and in the operations they perform. We focus here on lattice-based modular robots in which atoms are arranged on a regular grid. Crystalline robots [4] are one such example. A crystalline atom is a cubical device equipped with an expansion/contraction mechanism that allows it to extend each face out and retract it back. When extended, a face is twice as far from the cube's center when compared to its retracted distance. Each cube

face has an attachment mechanism that allows it to attach to (or detach from) adjacent atoms. When groups of atoms perform these operations (expand, contract, attach, detach) in a coordinated way, the atoms move relative to one another, resulting in a reconfiguration of the robot (see Fig. 1).

Several universal reconfiguration algorithms are available for transforming a crystalline robot from one configuration to another. Common to all is the requirement that atoms are grouped into *modules*.

In the most restricted model, where atoms are assumed to have fixed strength and are able to move only at fixed speed, any reconfiguration is possible in linear time, using modules of $2 \times 2 \times 2$ atoms. The total number of atom operations (counting multiple steps per time unit) is $O(n^2)$, and both bounds are worst-case optimal [2]. This model even restricts the communication range and on-board memory of each atom.

The total number of atom operations can be reduced to $O(n)$, although the static forces required may become linear instead of constant [1].

When constant force is required, but velocities are allowed to build up over time, reconfiguration is possible in $O(\sqrt{n})$ time in 2D, using the third dimension as an intermediate [9].

By removing all such assumptions and restrictions, any reconfiguration is possible in $O(\log n)$ time, using $O(n \log n)$ total operations; however, the module size increases to 32×32 for 2D reconfiguration [3]. A straightforward (yet unpublished) extension of this result achieves the same asymptotic bound in 3D, using larger but still constant-sized cube-shaped modules.

As far as we know, similar bounds for other lattice-based modular robots such as *Molecube* [15] and *M-TRAN* [7] are not yet known. In fact, we believe that most modular robots are capable of the same theoretical bounds, given an appropriate module design. For a comprehensive list of modular robot types, see [8, 13].

In this paper we show that M-TRAN and Molecube robots can also be efficiently reconfigured up to a scale factor. In other words, much like in previous work on Crystalline robots, reconfiguration assumes (and exploits) the existence of specifically constructed modules. Reconfiguration bounds apply to robots whose basic building block is such a module,

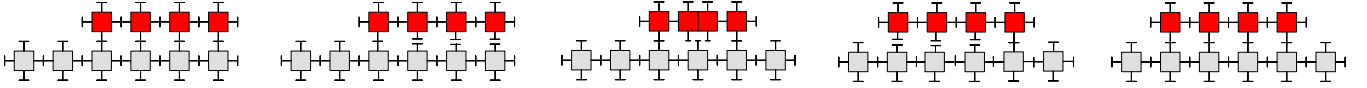


Fig. 1. Crystalline robot reconfiguration (2D example). Atoms can attach to neighbors, and expand/contract their arms. [Figure from [3].]

as opposed to the finer atoms themselves. Unlike most previous work, however, the modules we use are not space-filling.

Our method involves simulating a Crystalline atom with a module of M-TRAN or Molecube atoms. For both cases that we consider, the module shape has a six-arm structure, called a *6-arm*, that can simulate the operations of a crystalline *atom*. Thus, a robot constructed from 6-arms can reconfigure using any of the existing Crystalline algorithms (in fact the robot must be constructed from even larger modules of 6-arms, in accordance to the $k \times k \times k$ requirements in each existing Crystalline algorithm). We believe that the techniques developed here can be applied to other types of modular robots such as PolyBot G3 [12], Superbot [10, 5], RoomBot [11], and ATRON [6].

II. THE 6-ARM MODULE FOR M-TRAN AND MOLECUBE

A. M-TRAN and Molecube atoms

An M-TRAN atom [7] consists of two identical elements connected by a link. An element can be viewed as a half cube glued to a half cylinder, as depicted in Fig. 2a; the bounding box of an element is a unit cube.

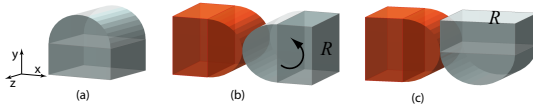


Fig. 2. The M-TRAN atom; (a) An M-TRAN element: front, back and bottom faces are equipped with attachment mechanisms; (b) Straight M-TRAN atom; (c) Bent M-TRAN atom.

An M-TRAN atom is equipped with six attachment mechanisms, one for each of its flat faces (three per element). Each element can rotate independently about its axis by $\pm 90^\circ$, so that any of the bounding box faces can have an attachment mechanism, if necessary. Fig. 2(b,c) shows two possible orientations of the two elements of an M-TRAN atom with respect to each other. We say that the M-TRAN atom sits in a *straight* position in Fig. 2b (all flat faces are vertical), and in a *bent* position in Fig. 2c. The arrow in Fig. 2b indicates the in-place 90° -rotation about the z -axis performed by the rotating right element, that leads to the bent position.

A Molecube atom [14, 15, 16] is a cubical structure (with rounded corners) equipped with a magnetic attachment mechanism on each of its faces. A diagonal cut extending from the top to the bottom face separates the cube into two triangular prisms (see Fig. 3a). This allows the atom to rotate its two halves about a symmetry axis orthogonal to the cut plane and passing through the center of the cube.

In both models, the rotating component temporarily exceeds its unit cell. However it never extends beyond half a unit in any direction.

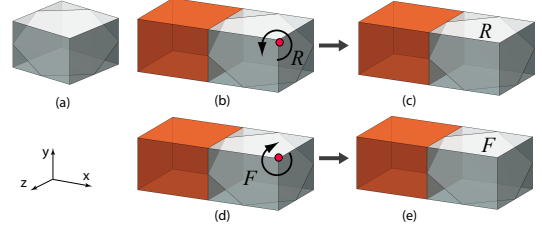


Fig. 3. (a) Molecube atom; (b→c) Transition of a Molecube block from straight to bent position through a counterclockwise rotation; (d→e) Clockwise rotation.

We define a Molecube *block* as two atoms attached face-to-face, as shown in Fig. 3b. The attachment is such that the axis of rotation for the right-hand atom is parallel to $(1, 1, 1)$.

A given face – say, the right face R , as shown in Fig. 3b – can rotate (by 120° counterclockwise) to an adjacent position as shown in Fig. 3c. Note that the transition depicted in Figures 3(b→c) is functionally similar to the transition depicted in Figures 2(b→c). As before, we refer to the configuration of the Molecube block from Fig. 3b as *straight*, and the configuration from Fig. 3c as *bent*. Figures 3(d→e) illustrate the effect of a clockwise rotation.

From this point on, we will simply refer to an M-TRAN atom as a block as well.

B. Design of 6-arm

We now show how to design a 6-arm that is suitable for M-TRAN and Molecubes. Recall that a 6-arm is meant to simulate the four Crystalline atom operations – expand, contract, attach and detach. Our structure¹ consists of six arms connected to a common $2 \times 2 \times 2$ *center piece* (see Fig. 4).

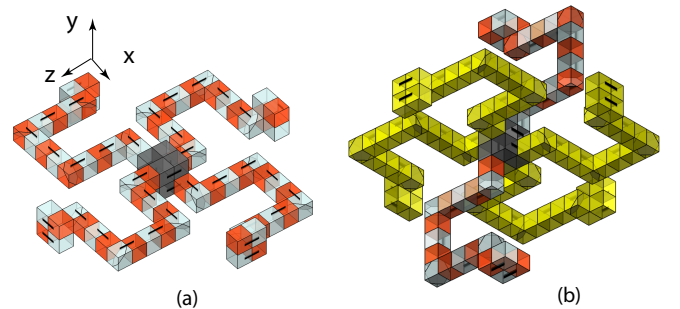


Fig. 4. A 6-arm module: (a) The four “horizontal” arms ; (b) entire structure from a different viewpoint (horizontal arms are now yellow).

Notice the alternating colors (red/white) of cubic components on the arms. This illustration is in accordance to

¹For additional material including animations, the reader may visit: <http://www.csc.villanova.edu/~mdamian/6arm>

Figures 2-3, and is meant to show adjacent elements (for M-TRAN) or atoms (for Molecube). Each block is marked by a black segment that connects a white cube to a red cube.

An arm can be viewed as a chain with four *joints*. A joint is a block which we allow to straighten and bend. An arm has two functional states: expanded and contracted (much like a Crystalline atom face). In an expanded state, all joints (and thus all blocks) of an arm are in a straight position (Fig. 5b for Molecubes and Fig. 6b for M-TRAN). In its contracted state, an arm forms a Π -shaped bend (Fig. 5a for Molecubes and Fig. 6a for M-TRAN). The tip of each arm occupies 2×2 cells and has an attachment mechanism that allows it to connect to an adjacent tip of another 6-arm.

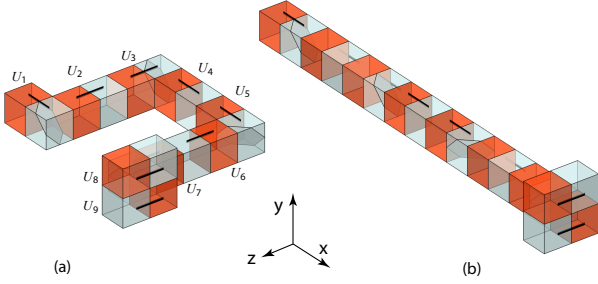


Fig. 5. (a) Contracted Molecube arm. U_1 attaches to the center piece of the 6-arm; (b) Extended arm.

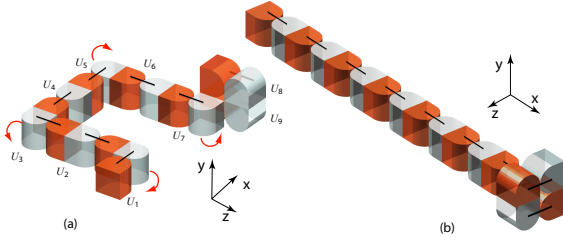


Fig. 6. (a) Contracted M-TRAN arm. U_1 attaches to the center piece of the 6-arm; (b) Extended arm.

Observe that when an arm is contracted, the distance from the tip to the center is 8 lattice units (7 along the arm, and 1 in the center piece). By simultaneously having joints U_1 , U_3 , U_5 , and U_7 straighten, the arm expands, doubling the distance from tip to center.

An arm expands by rotating (straightening) its joints in a coordinated way. By performing the four joint rotations simultaneously, we ensure that the tip attachment moves parallel to a coordinate axis. This is discussed in Section III.

Next we discuss the details of constructing an arm. Fix a coordinate system with the origin at the center of the $2 \times 2 \times 2$ center piece. Let the terms *right*, *left*, *top*, *bottom*, *front*, and *back* refer to the $+x$, $-x$, $+y$, $-y$, $+z$, $-z$ directions, respectively. For ease of presentation, we focus on the right arm only. As seen in Fig. 5a, it is composed of nine blocks U_1, \dots, U_9 , of which four behave as joints. The first eight blocks rest in a horizontal plane, whereas U_9 attaches directly above U_8 ; the reason for this particular attachment is to perfectly align the arm tip with the center piece. The center piece comprises

four blocks arranged in a $2 \times 2 \times 2$ configuration, as illustrated in Fig. 7. The four blocks are all in bent position, with the two right blocks oriented horizontally and the two left ones oriented vertically. The six attachment points for the arms are marked in Fig. 7b. Observe that the right arm attaches to the lower layer of the center piece, and thus by adding block U_9 above the main arm level the tip aligns with the center piece.

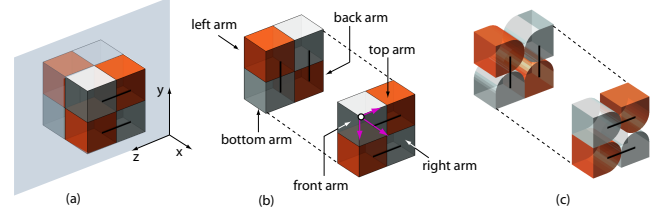


Fig. 7. (a) The center piece consists of four blocks in a $2 \times 2 \times 2$ grid of cells. (b) Molecube; (c) M-TRAN; The left and right halves of the center pieces are shown separated, with dotted lines indicating how the two halves attach in 3D. Attachment points for the arms are marked.

For M-TRAN, the orientation of blocks is straightforward, and can be seen easily in Fig. 6a. Each block is positioned so that an arm can only move within its initial plane.

For Molecubes, the situation is slightly more complicated. On a Molecube arm, the four joints are oriented so that the rotation axes of U_1 and U_3 are parallel, as are the rotation axes of U_5 and U_7 . To see that this is possible, notice that U_1 in Fig. 5a is an instance of the block shown in Fig. 3b that has been rotated by 90° clockwise (cw) about x ; U_3 is an instance of Fig. 3b that has been rotated by 90° counter-clockwise (ccw) about y . With these orientations, both joints have a rotation axis parallel to $(1, 1, -1)$.

To avoid collisions in the 6-arm, we have designed two variations of the Molecube arm. Fig. 8 illustrates the design of the right arm for Molecubes; we call this design a *type-A* arm. In a type-A arm, the rotation axis used by joints J_1 and J_3 is parallel to $(1, 1, -1)$, and the rotation axis used by J_5 and J_7 is parallel to $(1, -1, 1)$. Fig. 8b shows the arm position after J_1 and J_5 rotate by -60° and J_3 and J_7 rotate by 60° . Note that the tip of the arm has translated along the x -axis.

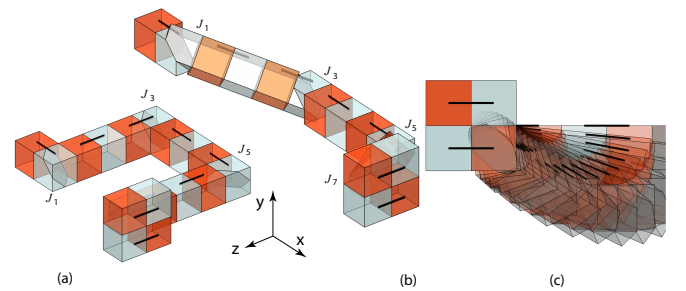


Fig. 8. Type-A Molecube right arm: (a) Contracted state; (b) After J_1 and J_5 rotate by angle -60° , while J_3 and J_7 rotate by 60° ; (c) Space swept by the arm through a rotation of 120° (view from $x = +\infty$).

An alternate design for the right arm is depicted in Fig. 9a; we will refer to this as a *type-B* arm. In the type-B arm, the rotation axis used by joints J_1 and J_3 is parallel to $(1, -1, -1)$,

and the rotation axis used by J_5 and J_7 is parallel to $(1, 1, 1)$. The arm extends by rotating its joints in directions opposite to those of a type-A arm. Fig. 9b shows the arm position after J_1 and J_5 rotate by 60° and J_3 and J_7 rotate by -60° .

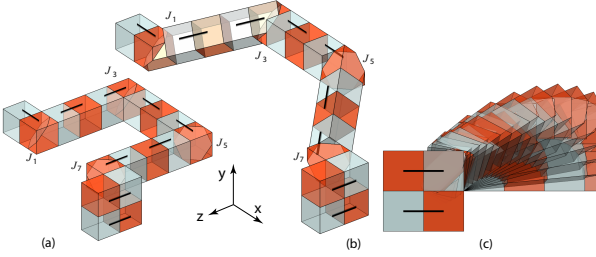


Fig. 9. Type-B Molecule right arm: (a) Contracted state; (b) After J_1 and J_5 rotate by 60° , while J_3 and J_7 rotate by -60° ; (c) Space swept by the arm through a rotation of 120° (view from $x = +\infty$).

The main difference between the type-A and type-B arms is the space swept during extension/contraction (see Fig. 8c vs. 9c). We carefully design the Molecube 6-arm so that the spaces swept by the six arms are disjoint and therefore no collisions occur. This is achieved as follows: the right and back arms are type-A, and the top, bottom, front and left arms are type-B.

Our 6-arm design works with both the Molecube and M-TRAN models, which differ only in the orientations of the rotation axes and the amount of rotation required for a joint to transition between its bent and straight positions.

III. SIMULATION OF CRYSTALLINE ATOM OPERATIONS

In this section we prove that a 6-arm can simulate the operations of a Crystalline atom.

For a fixed coordinate system, let $R_v(\theta)$ denote the 4×4 matrix that rotates a (homogeneous) point by θ degrees (ccw) about an axis parallel to the unit vector $v = (v_x, v_y, v_z)$ with fixed point at the origin. Let $T(d_x, d_y, d_z)$ denote the translation matrix that translates a point by d_x , d_y and d_z units in the directions x , y and z , respectively. Let J_i denote the rotating half of U_i , for $i = 1, 3, 5, 7$, and let O_i denote the center of J_i . We denote the x -coordinate of O_i by $x(O_i)$.

Lemma 1: Throughout the expansion/contraction of the right arm, the component connecting J_3 and J_5 remains parallel to the x -axis and does not rotate about O_3O_5 .

Proof: The matrix that determines the position and orientation of J_3 relative to O_1 is given by

$$R_a(-\theta)T(0, 0, -4)R_a(\theta) \quad (1)$$

where a is the rotation axis of J_1 and J_3 . For any axis a , the two rotations in the matrix product cancel each other out, and the net result is that J_3 undergoes only translational motion. This suffices for our proof because the component between J_3 and J_5 moves rigidly with J_3 . ■

The next lemma is very intuitive and its formal proof is given in the appendix.

Lemma 2: Throughout the expansion/contraction of the right arm, $x(O_1) \leq x(O_3) < x(O_5) \leq x(O_7)$.

Lemma 3: During the expansion/contraction of the right arm, the attachment at its tip moves parallel to the x -axis.

Proof: By Lemma 1, the midpoint m of the segment O_3O_5 undergoes a translation. Furthermore, by Lemma 2, this motion is x -monotone.

We can divide the arm into two halves, which are mirror images of each other, through a plane parallel to $x=0$, containing m . The second half can follow the motions of the first half symmetrically, in order to complete the desired motion.

Let a be the rotation axis for the first two joints, and b the axis for the last two joints. Let θ be the amount of rotation for each joint. Formally, the matrix that determines the position of J_7 relative to O_1 is

$$R_a(-\theta)T(0, 0, -4)R_a(\theta)T(4, 0, 0)R_b(-\theta)T(0, 0, 4)R_b(\theta) \quad (2)$$

Recall that we have chosen a and b to satisfy $(a_x, a_y, a_z) = (b_x, -b_y, -b_z)$. Then the product in equation (2) is a translation matrix having zero y - and z -components and a positive x -component. ■

Lemma 4: An arm does not self-intersect during expansion/contraction.

Proof: We prove the claim for the right arm. By Lemma 1, the segment O_3O_5 remains parallel to the x -axis throughout the arm motion, meaning that $x(O_3) + 4 = x(O_5)$. Along with Lemma 2, this implies that

$$x(O_1) + 4 \leq x(O_3) + 4 = x(O_5) \leq x(O_7)$$

Thus any pair of points in the set defined by the Cartesian product $\{O_1, O_3\} \times \{O_5, O_7\}$ are separated by at least 4 units in the x -dimension. This guarantees non self-intersection for the right arm. By symmetry, the arguments hold for the other arms as well. ■

Theorem 1: A 6-arm always remains inside the axis-aligned bounding box determined by the tips of its arms.

Proof: Our claim is equivalent to saying that the tip of the right arm is always the point with strictly maximum $+x$ coordinate. The range of the right tip is $8 \leq x \leq 16$. It suffices to show that no other arm ever enters the $x \geq 8$ halfplane.

The length of any arm is 15. One end of the arm is anchored to the center piece and the tip is constrained to a coordinate axis, by Lemma 3. Furthermore, by Lemma 1, the segment O_3O_5 is constrained to be parallel to this axis.

Therefore the arm is confined within a cylindrical region aligned with the coordinate axis, with radius strictly less than 6. Thus the cylindrical region avoids the $x \geq 8$ halfplane. ■

Define the *octant* of the right arm as the intersection of three halfplanes: $(x \geq 1, y \leq 1, z \leq 1)$. This contains the right arm in its contracted position. Notice that two of the octant boundary halfplanes are tangent to the arm tip, and all three are tangent to the center piece. The origin of the octant is on a corner of the center piece, on the same face but diagonally across the

connection of the right arm. The octant of each other arm can be defined symmetrically.

Lemma 5: An arm remains within its own octant during expansion/contraction.

Proof: We only focus on the expanding motion of the right arm in this proof. Other arms are handled symmetrically. First note that the right arm is type-A. Recall that, because it is horizontal, this means that some of its components will temporarily move downward.

By Lemma 2 and the fact that $x(O_1) = 2.5$, we know that the arm lies within the $x \geq 1$ halfplane.

Next we show that the right arm stays in the $z \leq 1$ halfplane. Consider an arm component between the rotating halves of two consecutive joints. Among all points on such a component, the point with the highest z -coordinate must lie on a joint (i.e., on one of the component endpoints). Thus, it suffices to focus only on the z -coordinates of joints (J_1, J_3, J_5, J_7) . Note that for any point $p \in J_1$, $z(p) \leq 1$. Also observe that, for any point $p \in J_3$, the value of $z(p)$ is no greater than 1 plus the z -translation component of the matrix

$$M_3 = R_a(-\theta)T(0, 0, -4)R_a(\theta) \quad (3)$$

Simple calculations (detailed in the Appendix) show that the z -component of M_3 is never greater than 0 for the values of a and θ restricted to the M-TRAN and the Molecube models. This implies that $z(p) \leq 1$ for any $p \in U_3$. By Lemma 1, the same holds true for $p \in U_5$. Finally, by Lemma 3 and the fact that U_7 is glued to the arm tip, we conclude that $z(p) < 1$, for any $p \in U_7$.

The calculations regarding the $y \leq 1$ constraint are similar. It can be verified that the y translation component of M_3 is never positive (see proof in the appendix). ■

Theorem 2: A 6-arm cannot self-intersect.

Proof: By Lemma 4, no arm self-intersects. By definition of the six octants, it can be verified that no octants intersect. By Lemma 5, this means that no two arms intersect. ■

Because a 6-arm always avoids self-intersection (Theorem 2), stays within the bounding box determined by its tips (Theorem 1), and each tip moves only along the normal of its axis-aligned face (Lemma 3), we conclude that an M-TRAN or Molecube 6-arm correctly simulates a Crystalline atom.

IV. EFFICIENCY OF 6-ARM RECONFIGURATION FOR M-TRAN AND MOLECUBES

We have established that a 6-arm simulates one Crystalline atom. Moreover, the number of atoms used to construct a 6-arm is constant, for both prototyped robots that we have considered. Thus any motion carried out by a 6-arm can be considered to use constant force and achieve constant velocities. In other words, our 6-arm construction does not affect any of the models considered in the literature. Let a 6-arm k -module be a $k \times k \times k$ collection of 6-arm modules. By substituting 6-arm modules for Crystalline modules, in prior work in the literature, we obtain identical *upper* bounds, while worst-case optimality is obtained in an almost identical way:

Theorem 3: [1] We can universally reconfigure n 6-arm 2-modules in $O(n)$ time using $O(n)$ operations.

We note here that the number of operations in Theorem 3 is asymptotically optimal in the worst case. In [1] this was demonstrated by a simple example of reconfiguring from a horizontal line to a vertical line. However, for M-TRAN and Molecube, this can be done in constant time. Instead, we can use the simple reconfiguration from all blocks straight, to an alternating straight-bent pattern. Then every other block must reconfigure.

Theorem 4: [3] We can universally reconfigure n 6-arm constant-size modules in $O(\log n)$ parallel steps and $O(n \log n)$ operations.² The number of parallel steps is optimal for labeled modules.

Theorem 5: [2] If only constant forces and velocities are allowed, we can universally reconfigure n 6-arm 2-modules in $O(n)$ parallel steps and $O(n^2)$ operations, and these bounds are optimal in the worst case. Furthermore, this can be done using only constant memory per atom, and with only local communication.

We note that the worst-case optimality cannot be deduced directly from [2], because we have only proved a one-way reduction. However, the same reasoning and example suffice: reconfiguring from a horizontal straight configuration to a vertical straight configuration. First, a constant fraction of the modules must change their vertical coordinate by an additive $\Omega(n)$, for a total change of $\Omega(n^2)$. Second, each constant-force operation changes the vertical coordinates of a constant number of modules by an additive constant, for a total change of $O(1)$. Therefore, the total number of operations must be at least the ratio $\Omega(n^2)$. Each parallel step can perform at most $O(n)$ operations (one per unit), so the total number of parallel steps must be $\Omega(n^2/n) = \Omega(n)$.

Theorem 6: [9] If constant forces are required (but velocity is unrestricted), we can universally reconfigure n 6-arm 2-modules in $O(\sqrt{n})$ time, using the third dimension as an intermediate.

V. COMMENTS AND FUTURE WORK

Our results show that certain modular robots can be reconfigured within the same asymptotic time bounds as Crystalline robots, provided an appropriate module structure is used. It remains interesting to construct smaller custom-made modules for each robot type, in hope of achieving the same bounds. It would also be interesting to use space-filling modules (densely filling a $k \times k \times k$ cube) or prove such a reduction impossible.

Another interesting question is whether any modular robot is fundamentally more powerful than Crystalline. Essentially this can be rephrased as asking whether any modular robot can reconfigure in $o(\log n)$ time, because other bounds seem to be tight for any model.

²The result in [3] is restricted to 2D and the constant is 32, but a straightforward extension applies to 3D. The best constant remains to be rigorously verified.

M-TRAN and Molecubes can be viewed as representative examples of two main types of hinge models. The former is edge-hinged and the latter is central-point-hinged.

We believe that several other (in particular, hinged) modular robots can be handled in the same way as presented here. In fact, our aim is to characterize a *generic block*, with a list of required properties that suffice for it to be used in the construction of a “global” 6-arm model. This will allow for a relatively simple way to verify that many modular robots can simulate Crystalline atoms. In fact, the number of specific atoms used to build the generic block will directly give the sufficient 6-arm module size in each case.

REFERENCES

- [1] G. Aloupis, S. Collette, M. Damian, E. D. Demaine, R. Flatland, S. Langerman, J. O’Rourke, S. Ramaswami, V. Sacristán, and S. Wuhler. Linear reconfiguration of cube-style modular robots. In *Proc. Intl. Symp. on Algorithms and Computation (ISAAC 2007)*, volume 4835 of *LNCS*, pages 208–219, 2007.
- [2] Greg Aloupis, Sébastien Collette, Mirela Damian, Erik D. Demaine, Dania El-Khechen, Robin Flatland, Stefan Langerman, Joseph O’Rourke, Val Pinciu, Suneeta Ramaswami, Vera Sacristán, and Stefanie Wuhler. Realistic reconfiguration of Crystalline and Telecube robots. In *8th International Workshop on the Algorithmic Foundations of Robotics (WAFR)*, 2008.
- [3] Greg Aloupis, Sébastien Collette, Erik D. Demaine, Stefan Langerman, Vera Sacristán, and Stefanie Wuhler. Reconfiguration of cube-style modular robots using $O(\log n)$ parallel moves. In *Proc. 19th Intl. Symp. on Algorithms and Computation (ISAAC)*, volume 5369 of *LNCS*, 2008.
- [4] Zack Butler, Robert Fitch, and Daniela Rus. Distributed control for unit-compressible robots: Goal-recognition, locomotion and splitting. *IEEE/ASME Trans. on Mechatronics*, 7(4):418–430, 2002.
- [5] Harris Chiu, Michael Rubenstein, and Wei-Min Shen. Multifunctional superbot with rolling track configuration. In *IROS’07: Workshop on Self-Reconfigurable Robots & Systems and Applications*, pages 50–53, November 2007.
- [6] Morten Winkler Jørgensen, Esben Hallundbæk Østergaard, and Henrik Hautop Lund. Modular ATRON: Modules for a self-reconfigurable robot. In *Proc. of the International Conference on Intelligent Robots and Systems*, pages 2068–2073, 2004.
- [7] Haruhisa Kurokawa, Kohji Tomita, Akiya Kamimura, Shigeru Kokaji, Takashi Hasuo, and Satoshi Murata. Self-reconfigurable modular robot m-tran: distributed control and communication. In *RoboComm ’07: Proceedings of the 1st international conference on Robot communication and coordination*, pages 1–7, Piscataway, NJ, USA, 2007. IEEE Press.
- [8] Satoshi Murata and Haruhisa Kurokawa. Self-reconfigurable robots: Shape-changing cellular robots can exceed conventional robot flexibility. *IEEE Robotics & Automation Magazine*, 14(1):43–52, 2007.
- [9] John H. Reif and Sam Slee. Optimal kinodynamic motion planning for self-reconfigurable robots between arbitrary 2D configurations. In *Robotics: Science and Systems Conference, Georgia Institute of Technology*, 2007.
- [10] Wei-Min Shen, Maks Krivokon, Harris Chiu, Jacob Everist, Michael Rubenstein, and Jagadeesh Venkatesh. Multimode locomotion via superbot reconfigurable robots. *Autonomous Robots*, 20(2):165–177, 2006.
- [11] Alexander Sproewitz, Aude Billard, Pierre Dillenbourg, and Auke Ijspeert. Roombots-mechanical design of self-reconfiguring modular robots for adaptive furniture. In *International Conference on Robotics and Automation*, 2009. To appear.
- [12] Mark Yim, Kimon Roufas, David Duff, Ying Zhang, Craig Eldershaw, and Sam Homans. Modular reconfigurable robots in space applications. *Auton. Robots*, 14(2-3):225–237, 2003.
- [13] Mark Yim, Wei-Min Shen, Behnam Salemi, Daniela Rus, Mark Moll, Hod Lipson, Eric Klavins, and Gregory S. Chirikjian. Modular self-reconfigurable robots systems: Challenges and opportunities for the future. *IEEE Robotics & Automation Magazine*, 14(1):43–52, 2007.
- [14] Victor Zykov, Andrew Chan, and Hod Lipson. Molecubes: An open-source modular robotics kit. In *IROS-2007 Self-Reconfigurable Robotics Workshop*, 2007.
- [15] Victor Zykov, Efstathios Mytilinaios, Bryant Adams, and Hod Lipson. Self-reproducing machines. *Nature*, 435(7038):163–164, 2005.
- [16] Victor Zykov, Phelps Williams, Nicolas Lassabe, and Hod Lipson. Molecubes extended: Diversifying capabilities of open-source modular robotics. In *IROS-2008 Self-Reconfigurable Robotics Workshop*, 2008.

APPENDIX

Proof of Lemma 2. Fix a coordinate system with origin at the center of the rotating half of U_1 . Then $x(U_1) = 0$ remains true throughout the expansion motion. The value of $x(U_3)$ is given by the x -translation component of the matrix $M_3 = R_a(-\theta)T(0, 0, -4)R_a(\theta)$ from (3). Recall that $a_z a_x = -1$ for Molecubes, and $a_z a_x = 0$ for M-TRAN. Thus

$$\begin{aligned} x(U_3) &= -4(1 - \cos(\theta))a_z a_x + 4\sin(\theta)a_y \\ &\geq -4(1 - \cos(\theta))a_z a_x \quad (\text{as } a_y \geq 0 \text{ and } \sin(\theta) \geq 0) \\ &\geq 0 \quad (\text{as } a_z a_x \leq 0 \text{ and } 1 - \cos(\theta) \geq 0) \end{aligned}$$

Thus we obtain the relation $x(U_1) \leq x(U_3)$. The value of $x(U_5)$ is given by the x -translation component of the matrix $M_3 T(4, 0, 0) R_b(-\theta)$, which shows that $x(U_5) = x(U_3) + 4$. Finally, $x(U_7)$ is given by the x translation component of $R_a(-\theta)T(0, 0, -4)R_a(\theta)T(4, 0, 0)R_b(-\theta)T(0, 0, 4)R_b(\theta)$.

It can be shown that

$$\begin{aligned} x(U_7) &= -8a_z a_x + 8\cos(\theta)a_z a_x + 8\sin(\theta)a_y + 4 \\ &= 2 * x(U_3) + 4 \\ &= x(U_5) + x(U_3) \\ &\geq x(U_5) \quad (\text{as } x(U_3) \geq 0) \end{aligned}$$

Proof of Lemma 5. We show that the z -translation component of the matrix from (3) is always less than or equal to 0. Call this component Z_3 . The value of Z_3 is given by the z -translation component from (3):

$$Z_3 = -4(\cos(\theta) + (1 - \cos(\theta))a_z^2)$$

It can be easily verified that $Z_3 \leq 0$ for the values of a_z and θ imposed by the Molecube and M-TRAN models.

Next we show that the y -translation component of the matrix from (3) is always less than or equal to 0. Call this component Y_3 . The value of Y_3 is given by the y -translation component from (3):

$$Y_3 = -4((1 - \cos(\theta))a_z a_y + \sin(\theta))a_x$$

It can be easily verified that $Y_3 \leq 0$ for the values of a and θ imposed by the Molecube and M-TRAN models.